Isolation of a Chloride-Capped Cerium Polyoxo Nanocluster Built from 52 Metal Ions

Anamar Blanes-Díaz,[a] Jennifer N. Wacker,[a,b] Jennifer E. S. Szymanowski,[c] Jeffery A. Bertke,[a] and Karah E. Knope*[a]

* To whom correspondence should be addressed: kek44@georgetown.edu

ELECTRONIC SUPPLEMENTARY INFORMATION

TABLE OF CONTENTS

Synthesis of Cerium Phases

Materials

All materials were purchased from commercial suppliers and used as received. Ceric ammonium nitrate ($(NH_4)_2Ce(NO_3)_6$; Baker Analyzed Reagent, J.T. Baker Chemical Co.), hydrochloric acid ($HCl_{(aq)}$; Fisher Scientific), pyridine (Fisher Scientific), and ammonium hydroxide (NH_4OH; Fisher Scientific). Acid solutions were prepared by diluting concentrated hydrochloric acid with nanopure water (18.2 MΩ·cm; Millipore, USA).

$(NH_4)_2Ce(NO_3)_6$ (0.247-0.274 g; ~0.5 mmol) was dissolved in water (approximately 0.5 M in Ce^{4+}). Excess $NH_4OH_{(aq)}$ was added to yield a yellow precipitate. The mixture was centrifuged, and the supernatant was discarded. After washing with water (2 × 2 mL), the yellow pellet was dissolved in $HCl_{(aq)}$ (1 mL; 1 M). Complete dissolution of the pellet occurred over several hours. An aliquot of this acidic $Ce_{(aq)}$ stock solution (25 μL; ~0.013 mmol in Ce; ~7 mg of Ce) was subsequently combined with HCl (200 μL; 1 M) and pyridine (5 μL; 0.062 mmol) in a 3 mL shell vial; the resulting solution was pale-yellow. The reaction solution was allowed to slowly evaporate over several days under ambient conditions in a fume hood. When the solution had gone almost completely to dryness (approximately 50 μL of the reaction solution remained), a few dark yellow parallelograms (50 μm approximate diameter) were observable under an optical microscope and determined by single crystal X-ray diffraction to be $(HPy)_m[Ce_{52}O_{80-x}(OH)_xCl_{59}(H_2O)_{17}]\cdot nH_2O$, **Ce52**. Typically, on the order of 5–20 crystals of **Ce52** would precipitate from the reaction solution. Note that small changes in the reaction conditions also yielded $(HPy)_m[Ce_{38}O_{56-x}(OH)_xCl_{50}(H_2O)_{12}]\bullet nH_2O$ (**Ce38**) and two phases consisting of $CeCl_6^{2-}$ including $(HPy)_2[CeCl_6]\cdot 2(HPyCl)$ (**Ce1-1**) and $HPy_2[CeCl_6]$ (**Ce1-2**).

As the reaction was carried out using slow evaporation under ambient conditions, crystallization was dependent on factors such as humidity and temperature as crystals were obtained when the solution had gone to almost complete dryness.

Crystallographic Structure Refinement Details

The structures for compounds **Ce1-1, Ce1-2, Ce38,** and **Ce52** were determined using single crystal X-ray diffraction on a Bruker Quest D8 diffractometer equipped with a IμS X-ray source (Mo Kα radiation; λ=0.71073) and a CMOS detector. Single crystals were isolated from the bulk reaction products and mounted on MiTeGen Micromounts™. Data were collected at 100(2) K and the APEX III software suite was used to identify unit cells, integrate the data, and apply absorption corrections.[1] The structures were solved using intrinsic phasing methods and refined using *SHELXL*[2] within the *ShelXle*[3] graphical user interface. Crystallographic refinement details for the reported compounds can be found in Table S1.

Table S1. Crystallographic refinement details for compounds **Ce1-1**, **Ce1-2**, **Ce38**, and **Ce52**

	Ce1-1	**Ce1-2**	**Ce38**	**Ce52**
formula	$C_{20}H_{24}CeCl_8N_4$	$C_{10}H_{12}CeCl_6N_2$	$C_{20}H_{24}Ce_{38}Cl_{50}N_4O_{92}$	$Ce_{52}Cl_{58}O_{98}$; $Ce_{52}Cl_{60}O_{96}$
MW (g mol^{-1})	744.15	513.04	8889.49	21859.58
T (K)	100(2)	100(2)	100(2)	100(2)

crystal color/ habit	yellow	yellow	yellow	yellow
crystal system	triclinic	monoclinic	monoclinic	monoclinic
space group	*P-1*	*C2/m*	$P2_1/n$	*P2/m*
λ (Å)	0.71073	0.71073	0.71073	0.71073
a (Å)	7.5899(6)	12.9930(6)	18.8106(7)	22.2147(10)
b (Å)	9.2556(8)	8.6538(4)	18.7789(7)	29.7354(14)
c (Å)	11.8931(9)	7.9621(3)	28.4413(11)	24.3598(12)
α (deg)	100.578(2)	90	90	90
β (deg)	104.990(3)	97.8270(10)	97.6020(10)	102.3645(14)
γ (deg)	107.349(2)	90	90	90
Volume (Å^3)	738.90(10)	886.91(7)	9958.4(7)	15717.9(13)
Z	1	2	2	1
ρ (mg m^{-3})	1.672	1.921	2.965	2.309
μ (mm^{-1})	2.280	3.457	9.219	7.894
R_1	0.0267	0.0217	0.0544	0.0716
wR_2	0.0600	0.0607	0.1188	0.2061
GOF	1.166	1.073	1.012	1.036
CCDC	2359377	2359378	2359379	2359380

Refinement details Ce1-1, $(HPy)_2[CeCl_6]\cdot 2(HPyCl)$

Rigid-bond restraints were imposed on displacement parameters for all atoms. A structural model consisting of one half of the $(HPy)_2[CeCl_6]\cdot 2(HPyCl)$ per asymmetric unit was developed. All Cl coordinated to Ce are disordered over two positions. The like Ce-Cl distances were restrained to be similar (esd 0.01Å). The lattice Cl is disordered over two positions. Both pyridinium cations are disordered over two orientations. The like C-N and C-C distances have been restrained to be similar. The Cl1B,Cl4, and Cl4B atoms were restrained to behave relatively isotropic. Similar displacement amplitudes (esd 0.01) were imposed on disordered sites overlapping by less than the sum of van der Waals radii. The pyridinium hydrogen atoms were located in the difference map. The N-H distances were restrained to be 0.86 (0.02 Å). Remaining H atoms were included as riding idealized contributors. Pyridinium H atom U's were assigned as 1.5 times U_{eq} of the carrier atom; remaining H atom U's were assigned as 1.2 times carrier U_{eq}

Refinement details Ce1-2, $HPy_2[CeCl_6]$

A structural model consisting of 1/4 of the target $CeCl_6^{2-}$ anion and 1/2 of a pyridinium cation per asymmetric unit was developed. The cation is disordered over two positions across a symmetry site. The rings were constrained to be ideal hexagons. Similar displacement amplitudes (esd 0.01) were imposed on disordered sites overlapping by less than the sum of van der Waals radii.

The pyridinium N-H hydrogen atoms could not be located in the difference map and thus were placed in calculated positions. The remaining H atoms were included as riding idealized contributors. H atom U's were assigned as 1.2 times carrier U_{eq}.

Refinement details Ce38, $(HPy)_m[Ce_{38}O_{56-x}(OH)_xCl_{50}(H_2O)_{12}]\bullet nH_2O$

A structural model consisting of one half of the cluster plus 87 disordered water solvate molecules per asymmetric unit was developed; however, positions for the idealized solvate molecules were poorly determined. Since positions for the solvate molecules were poorly determined a second structural model was refined with contributions from the solvate molecules removed from the diffraction data using the bypass procedure in PLATON (Spek, 2015). No positions for the host network differed by more than two su's between these two refined models. The electron count from the "squeeze" model converged in good agreement with the number of solvate molecules predicted by the complete refinement. The "squeeze" data are reported here.

H atoms were included as riding idealized contributors. H atom U's were assigned as 1.2 times carrier U_{eq}. Water and hydroxyl H atoms could not be located in the difference map and thus were left off of the model.

Both pyridinium molecules are disordered over two orientations. The like C-C and N-C distances were restrained to be similar (esd 0.01 Å). Similar displacement amplitudes (esd 0.01) were imposed on disordered sites overlapping by less than the sum of van der Waals radii. Several atoms were restrained to behave relatively isotropic

Refinement details Ce52, $(HPy)_m[Ce_{52}O_{80-x}(OH)_xCl_{59}(H_2O)_{17}]\cdot nH_2O$

A structural model consisting of the cluster plus 616 disordered water solvate molecules was developed; however, positions for the idealized solvate molecules were poorly determined. Since positions for the solvate molecules could not be determined a second structural model was refined with contributions from the solvate molecules removed from the diffraction data using the bypass procedure in PLATON (Spek, 2015). No positions for the host network differed by more than two su's between these two refined models. The electron count from the "squeeze" model converged in good agreement with the number of solvate molecules predicted by the complete refinement. The "squeeze" data are reported here.

Five chloride ligands are disordered over two orientations. The like Ce-Cl distances were restrained to be similar (esd 0.01 Å). Rigid-bond restraints were imposed on displacement parameters for all sites and similar displacement amplitudes (esd 0.01) were imposed on disordered sites overlapping by less than the sum of van der Waals radii. In order for the model to converge, the core oxygen atoms of "cluster 2" were constrained to have equal anisotropic displacement parameters.

Hydrogen atoms on the water/hydroxyl oxygen atoms could not be located in the difference map and thus were left off of the model. A total of twelve reflections were omitted from the final refinement because they were partially obscured by the shadow of the beamstop.

ORTEP Diagrams

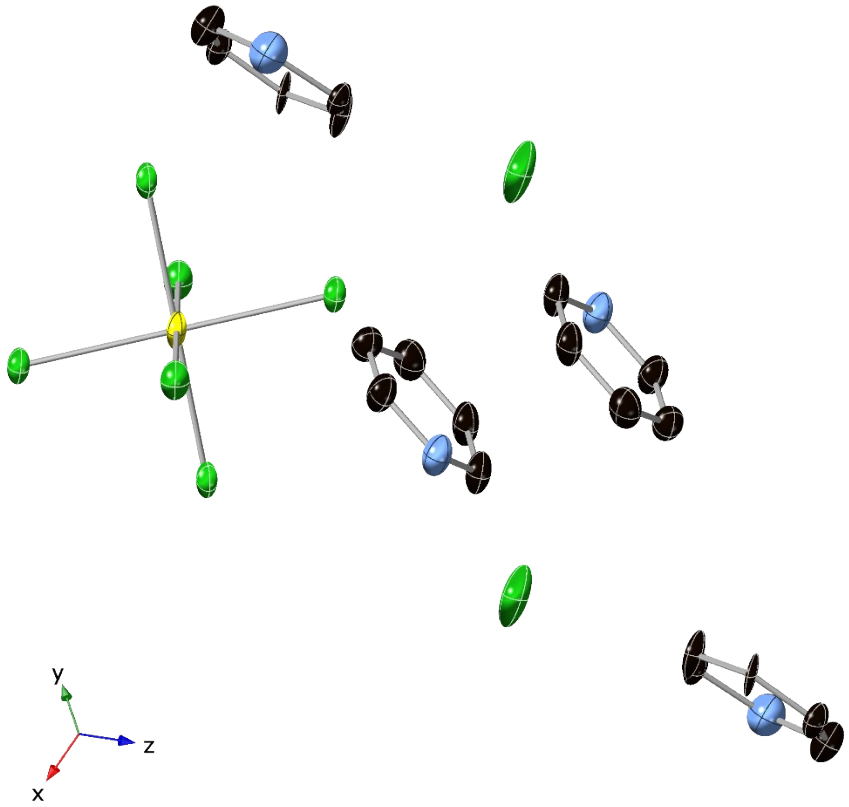

Figure S3. ORTEP illustration of **Ce1-1** shown at the 50% probability level at 100(2) K. The color scheme is as follows: Ce (yellow), Cl (green), C (black), and N (blue). Hydrogen atoms and disorder have been omitted for clarity.

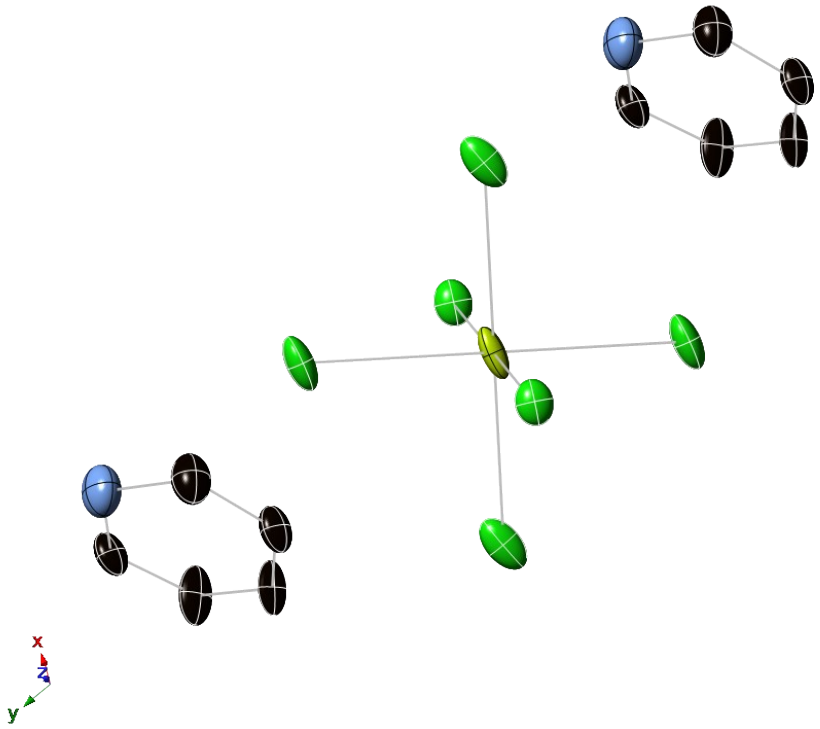

Figure S4. ORTEP illustration of **Ce1-2** shown at the 50% probability level at 100(2) K. The color scheme is as follows: Ce (yellow), Cl (green), C (black), and N (blue). Hydrogen atoms and disorder have been omitted for clarity.

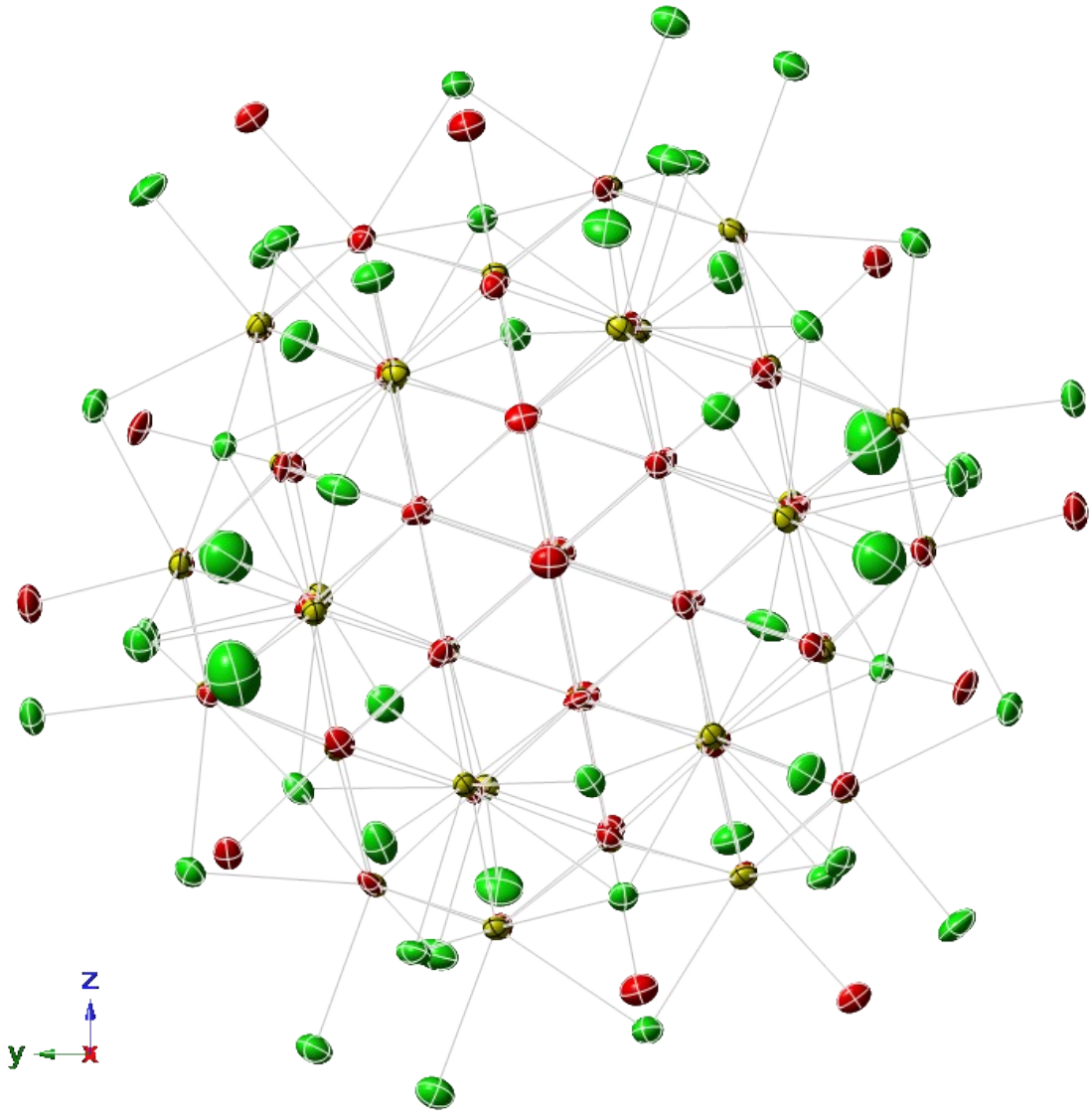

Figure S5. ORTEP illustration of **Ce38** shown at the 50% probability level at 100(2) K. The color scheme is as follows: Ce (yellow), Cl (green), O (red). Hydrogen atoms and disorder have been omitted for clarity. Outer sphere waters and pyridinium ions were squeezed from the structure and not shown.

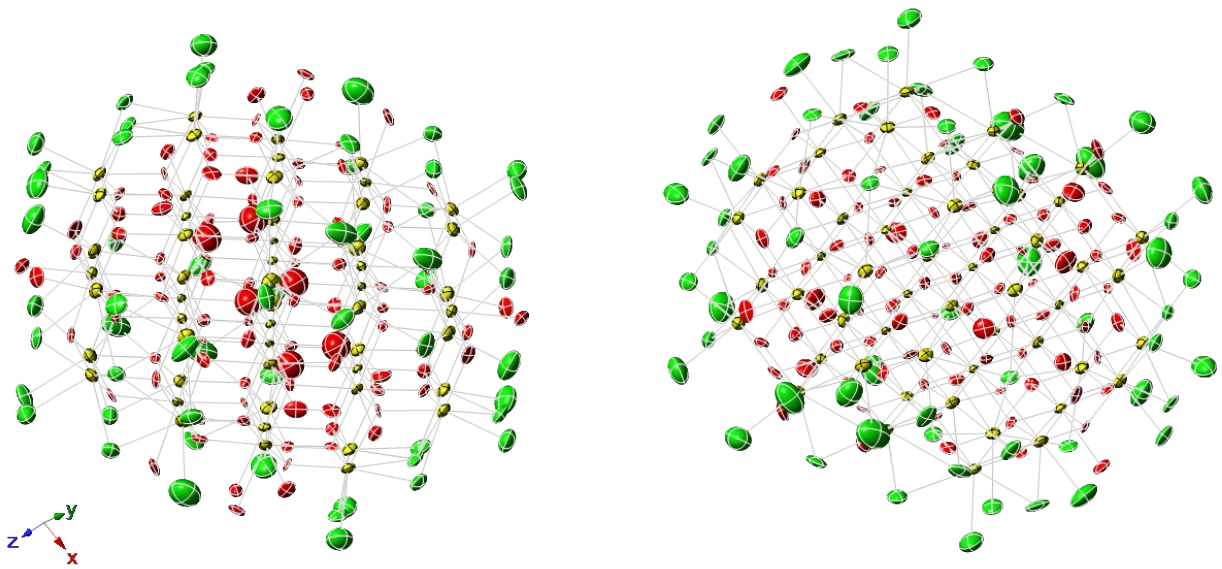

Figure S6. ORTEP illustration of **Ce52** shown at the 50% probability level at 100(2) K. There are two distinct clusters in **Ce52**. The color scheme is as follows: Ce (yellow), Cl (green), O (red). Hydrogen atoms and disorder have been omitted for clarity. Outer sphere waters and pyridinium ions were squeezed from the structure and not shown.

Structure descriptions

Ce1-1; $(HPy)_2[CeCl_6]\cdot 2(HPyCl)$

Compound **Ce1-1** is composed of a monomeric $CeCl_6^{2-}$ unit stabilized by two pyridinium counterions. There are also two pyridinium and two chloride ions in the outer coordination sphere. The average Ce-Cl bond distance for this compound is 2.62(4) Å.

Ce1-2; $(HPy)_2[CeCl_6]$

Compound **Ce1-2** is composed of a monomeric $CeCl_6^{2-}$ unit stabilized by two pyridinium counterions, similar to that of **Ce1-1**. However, there are no other outer sphere counterions present in this structure. The average Ce-Cl bond distance is 2.60(11) Å, similar to **Ce1-1**.

Ce38; $(HPy)_m[Ce_{38}O_{56-x}(OH)_xCl_{50}(H_2O)_{12}]\bullet nH_2O$

The structure of **Ce38** is related to that of the previously reported{Ce_{38}} by our group.[4] The cluster core of **Ce38** consists of 38 cerium atoms bridged by 56 μ_3– and μ_4–oxo anions groups. The surface of the cluster is decorated with 50 chloride and 12 water ligands that cap the cluster core. A deeper look into the cluster core reveals a {Ce_{14}} core of cubic, 8-coordinate CeO_8 that adopts a fluorite structure. There are 7 unique Ce sites that, together with their symmetry equivalents, make up the {Ce_{14}} core. This core is then capped by 6 {Ce_4} caps that composed of 12 unique Ce sites and their symmetry equivalents.

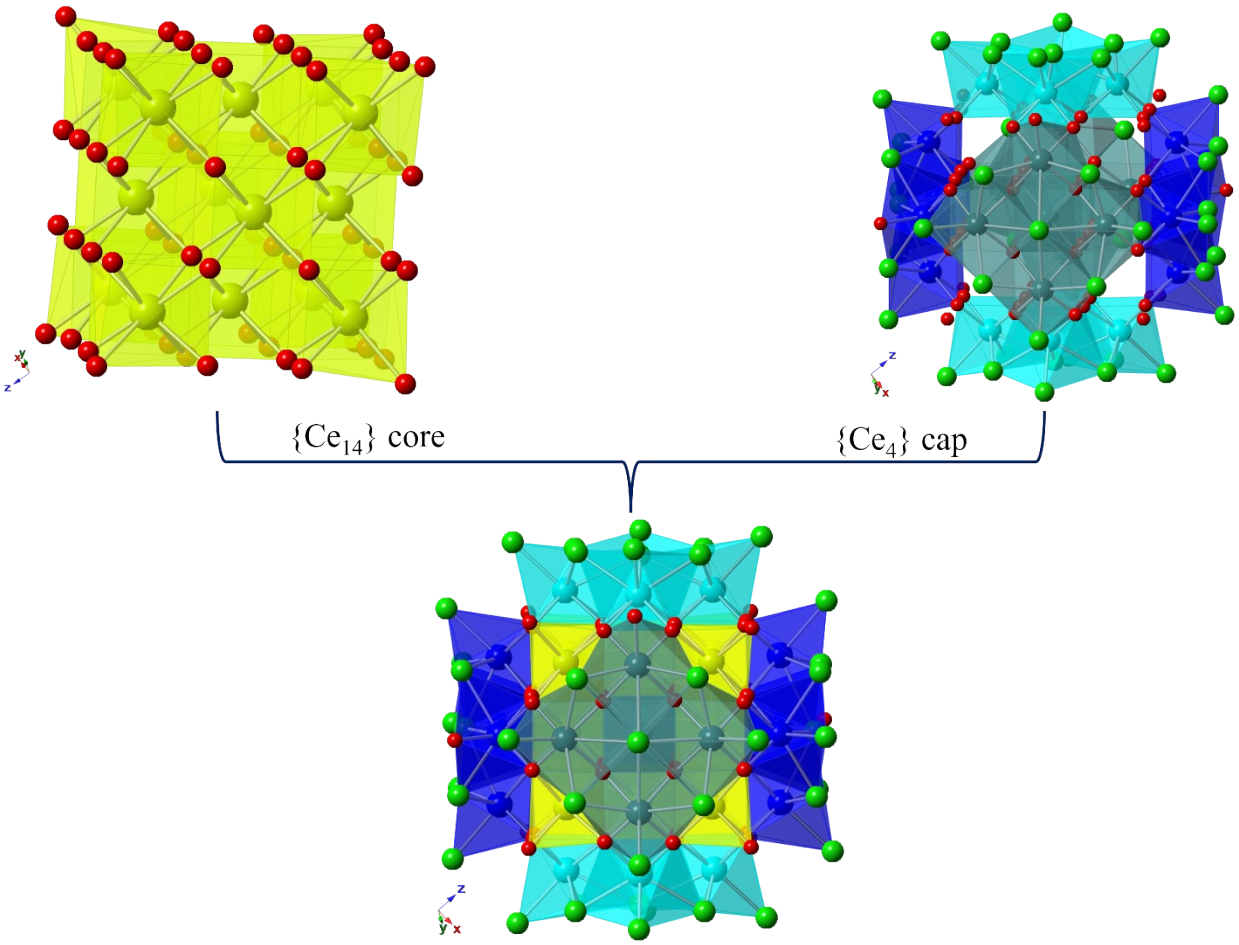

Figure S7. The {Ce_{14}} core and 6x {Ce_4} caps that make up **Ce38**. The atoms are color coded for ease. Ce atoms are yellow, blue, turquoise, and teal, O are in red, and Cl are in green. The {Ce_4} caps are colored differently (blue, turquoise, and teal) for ease.

Ce52; $(HPy)_m[Ce_{52}O_{80-x}(OH)_xCl_{59}(H_2O)_{17}]\cdot nH_2O$

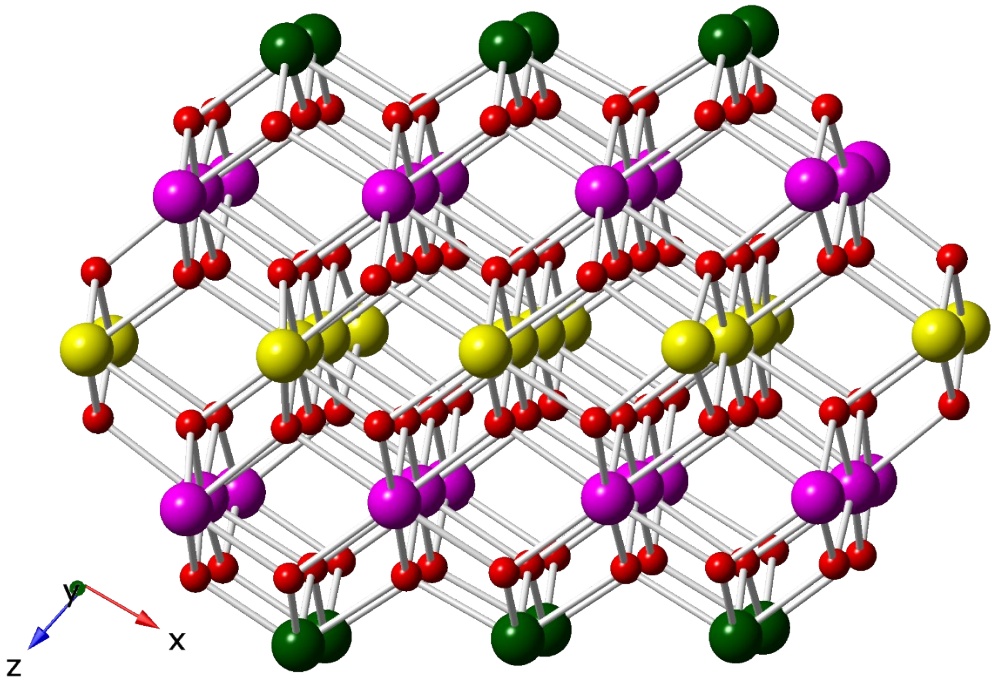

Figure S8. Ball and stick representation of **Ce52** without surface Cl^- and H_2O ligands showcasing the A:B:C:B:A layers. Ce atoms are colored as follows to display the different layers: A- green, B- pink, C- yellow.

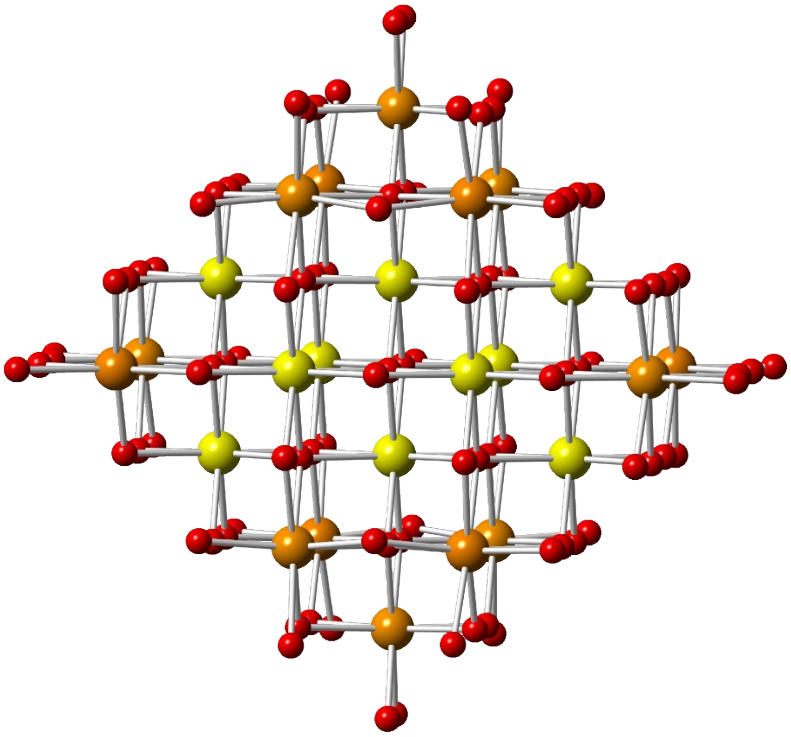

Figure S9. The {Ce_{24}} core of **Ce52** with the 10 CeO_8 sites in yellow and the remaining 14 Ce sites, coordinated to both O and H_2O, in orange.

Bond Valence Summation Values

Bond valence summation values were calculated using the equation $v_{ij} = \exp[(R_{ij}-d_{ij})/b)]$ where v_{ij} is the individual valence, d_{ij} is the bond length between *i* and *j*, R_{ij} is the bond valence parameter, and b is a constant. All of the individual valences are added to obtain the overall valence for a particular atom.

Ambiguous values prevented from making a definitive assignment of the oxidation states for Ce atoms within the clusters. However, UV-vis-NIR data for **Ce52** was consistent with a mixed valent cluster.

Table S2. Cerium bond valence summation values for **Ce38**. Calculations performed using R_{ij} (Ce^{IV}-Cl) from Brese, N. E. and O'Keeffe, M. **1991** and R_{ij} ($Ce^{III/IV}$-O) from Roulhac, P. L. and Palenik, G. J. **2003**.[5, 6]

Atom	Ce BVS	Assignment	Atom	Ce BVS	Assignment
Ce1	4.12	Ce^{IV}	**Ce11**	3.95	Ce^{IV}
Ce2	3.93	Ce^{IV}	**Ce12**	4.13	Ce^{IV}
Ce3	3.94	Ce^{IV}	**Ce13**	4.05	Ce^{IV}
Ce4	3.99	Ce^{IV}	**Ce14**	3.95	Ce^{IV}
Ce5	3.92	Ce^{IV}	**Ce15**	3.94	Ce^{IV}
Ce6	3.85	Ce^{III}/Ce^{IV}	**Ce16**	4.00	Ce^{IV}

Ce7	4.03	Ce^{IV}	**Ce17**	3.90	Ce^{IV}
Ce8	3.91	Ce^{IV}	**Ce18**	3.93	Ce^{IV}
Ce9	4.09	Ce^{IV}	**Ce19**	4.10	Ce^{IV}
Ce10	3.92	Ce^{IV}			

Intermediary values suggest the contribution of both Ce^{III} and Ce^{IV}.

Table S3. Cerium bond valence summation values for **Ce38** using R_{ij} (Ce^{IV}-O) from Trzesowska, A.; Kruszynski, R.; Bartczak, T. J. **2006** and R_{ij} (Ce^{IV}-Cl) from Brese, N. E. and O'Keeffe, M. **1991**.[6, 7]

Atom	BVS	Atom	BVS	Atom	BVS
Ce1	3.91	**Ce8**	3.78	**Ce15**	3.73
Ce2	3.79	**Ce9**	3.93	**Ce16**	3.79
Ce3	3.80	**Ce10**	3.77	**Ce17**	3.72
Ce4	3.86	**Ce11**	3.81	**Ce18**	3.80
Ce5	3.79	**Ce12**	3.91	**Ce19**	3.95
Ce6	3.70	**Ce13**	3.85		
Ce7	4.44	**Ce14**	3.75		

Table S4. Cerium bond valence summation values for **Ce38** using R_{ij} (Ce^{IV}-O) and (Ce^{IV}-Cl) from Brese, N. E. and O'Keeffe, M. **1991**.[6]

Atom	BVS	Atom	BVS	Atom	BVS
Ce1	3.46	**Ce8**	3.48	**Ce15**	3.30
Ce2	3.49	**Ce9**	3.63	**Ce16**	3.35
Ce3	3.51	**Ce10**	3.48	**Ce17**	3.28
Ce4	3.56	**Ce11**	3.51	**Ce18**	3.45
Ce5	3.49	**Ce12**	3.45	**Ce19**	3.65
Ce6	3.41	**Ce13**	3.40		
Ce7	4.14	**Ce14**	3.31		

Table S5: Oxygen bond valence summation values for **Ce38.** Calculations performed using R_{ij} ($Ce^{III/IV}$-O) from Roulhac, P. L. and Palenik, G. J. **2003**.[5]

Atom	BVS	Assignment	Atom	BVS	Assignment	Atom	BVS	Assignment
O1	2.13	μ_4-oxo	**O13**	2.15	μ_3-oxo	**O25**	0.34	H_2O
O2	2.00	μ_4-oxo	**O14**	2.09	μ_4-oxo	**O26**	2.12	μ_4-oxo
O3	2.11	μ_4-oxo	**O15**	2.12	μ_3-oxo	**O27**	0.36	H_2O
O4	1.65	μ_3-oxo	**O16**	2.15	μ_3-oxo	**O28**	2.13	μ_3-oxo
O5	2.10	μ_4-oxo	**O17**	2.19	μ_3-oxo	**O29**	0.40	H_2O
O6	2.11	μ_4-oxo	**O18**	2.13	μ_4-oxo	**O30**	2.11	μ_3-oxo
O7	2.12	μ_4-oxo	**O19**	2.14	μ_3-oxo	**O32**	1.99	μ_4-oxo
O8	2.11	μ_3-oxo	**O20**	2.09	μ_3-oxo	**O33**	0.30	H_2O

O9	1.98	μ_4-oxo	**O21**	0.38	H_2O	**O34**	1.99	μ_4-oxo
O10	2.10	μ_3-oxo	**O22**	2.12	μ_4-oxo	**O36**	2.16	μ_3-oxo
O11	2.13	μ_3-oxo	**O23**	0.35	H_2O			
O12	2.11	μ_4-oxo	**O24**	2.12	μ_4-oxo			

Table S6. Cerium bond valence summation values for **Ce52**. Calculation performed using R_{ij} (Ce^{IV}-Cl) from Brese, N. E. and O'Keeffe, M. **1991** and R_{ij} ($Ce^{III/IV}$-O) from Roulhac, P. L. and Palenik, G. J. **2003**.[5, 6]

Atom	Ce BVS	Assignment	Atom	Ce BVS	Assignment
Ce1	3.92	Ce^{IV}	**Ce18**	3.70	Ce^{III}/Ce^{IV}
Ce2	3.83	Ce^{III}/Ce^{IV}	**Ce19**	4.15	Ce^{IV}
Ce3	3.80	Ce^{III}/Ce^{IV}	**Ce20**	4.14	Ce^{IV}
Ce4	4.22	Ce^{IV}	**Ce21**	4.04	Ce^{IV}
Ce5	3.92	Ce^{IV}	**Ce22**	3.83	Ce^{III}/Ce^{IV}
Ce6	4.03	Ce^{IV}	**Ce23**	3.87	Ce^{III}/Ce^{IV}
Ce7	3.79	Ce^{III}/Ce^{IV}	**Ce24**	4.21	Ce^{IV}
Ce8	4.03	Ce^{IV}	**Ce25**	4.23	Ce^{IV}
Ce9	4.26	Ce^{IV}	**Ce26**	4.02	Ce^{IV}
Ce10	3.83	Ce^{III}/Ce^{IV}	**Ce27**	3.94	Ce^{IV}
Ce11	4.34	Ce^{IV}	**Ce28**	4.00	Ce^{IV}
Ce12	4.03	Ce^{IV}	**Ce29**	4.15	Ce^{IV}
Ce13	4.08	Ce^{IV}	**Ce30**	3.70	Ce^{III}/Ce^{IV}
Ce14	3.88	Ce^{III}/Ce^{IV}	**Ce31**	4.02	Ce^{IV}
Ce15	3.95	Ce^{IV}	**Ce32**	3.87	Ce^{III}/Ce^{IV}
Ce16	3.92	Ce^{IV}	**Ce33**	3.84	Ce^{III}/Ce^{IV}
Ce17	3.99	Ce^{IV}			

Intermediary values suggest contributions from both Ce^{III} and Ce^{IV}.

Table S7. Cerium bond valence summation values for **Ce52** using R_{ij} (Ce^{IV}-O) from Trzesowska, A.; Kruszynski, R.; Bartczak, T. J. **2006** and R_{ij} (Ce^{IV}-Cl) from Brese, N. E. and O'Keeffe, M. **1991**.[6, 7]

Atom	BVS	Atom	BVS	Atom	BVS
Ce1	3.79	**Ce12**	3.82	**Ce23**	3.67
Ce2	3.69	**Ce13**	3.87	**Ce24**	3.99
Ce3	3.60	**Ce14**	3.68	**Ce25**	4.01
Ce4	3.99	**Ce15**	3.81	**Ce26**	3.81
Ce5	3.78	**Ce16**	3.71	**Ce27**	3.80
Ce6	3.88	**Ce17**	3.84	**Ce28**	3.86
Ce7	3.65	**Ce18**	3.56	**Ce29**	3.93

Ce8	3.81	**Ce19**	3.94	**Ce30**	3.57
Ce9	4.04	**Ce20**	3.99	**Ce31**	3.88
Ce10	3.69	**Ce21**	3.83	**Ce32**	3.66
Ce11	4.11	**Ce22**	3.69	**Ce33**	4.06

Table S8. Cerium bond valence summation values for **Ce52** using R_{ij} (Ce^{IV}-O) and (Ce^{IV}-Cl) from Brese, N. E. and O'Keeffe, M. **1991**.[6]

Atom	BVS	Atom	BVS	Atom	BVS
Ce1	3.50	**Ce12**	3.37	**Ce23**	3.24
Ce2	3.40	**Ce13**	3.41	**Ce24**	3.52
Ce3	3.18	**Ce14**	3.25	**Ce25**	3.54
Ce4	3.53	**Ce15**	3.51	**Ce26**	3.36
Ce5	3.48	**Ce16**	3.28	**Ce27**	3.49
Ce6	3.56	**Ce17**	3.53	**Ce28**	3.56
Ce7	3.37	**Ce18**	3.28	**Ce29**	3.47
Ce8	3.37	**Ce19**	3.48	**Ce30**	3.29
Ce9	3.57	**Ce20**	3.67	**Ce31**	3.57
Ce10	3.39	**Ce21**	3.38	**Ce32**	3.24
Ce11	3.63	**Ce22**	3.40	**Ce33**	3.76

Table S9. Oxygen bond valence summation values for **Ce52.** Calculations performed using R_{ij} ($Ce^{III/IV}$-O) from Roulhac, P. L. and Palenik, G. J. **2003**.[5]

Atom	BVS	Assignment	Atom	BVS	Assignment	Atom	BVS	Assignment
O1	2.10	μ_4-oxo	**O20**	2.09	μ_4-oxo	**O39**	0.37	H_2O
O2	2.11	μ_4-oxo	**O21**	2.07	μ_3-oxo	**O40**	2.05	μ_3-oxo
O3	2.14	μ_4-oxo	**O22**	2.15	μ_4-oxo	**O41**	2.10	μ_3-oxo
O4	2.17	μ_4-oxo	**O23**	2.16	μ_4-oxo	**O42**	2.15	μ_4-oxo
O5	2.03	μ_4-oxo	**O24**	2.05	μ_3-oxo	**O43**	0.35	H_2O
O6	2.01	μ_4-oxo	**O25**	2.11	μ_4-oxo	**O44**	2.06	μ_3-oxo
O7	2.02	μ_4-oxo	**O26**	2.14	μ_4-oxo	**O45**	2.14	μ_3-oxo
O8	2.03	μ_4-oxo	**O27**	2.16	μ_4-oxo	**O46**	2.09	μ_3-oxo
O9	2.14	μ_4-oxo	**O28**	2.10	μ_4-oxo	**O47**	0.29	H_2O
O10	2.02	μ_4-oxo	**O29**	2.03	μ_4-oxo	**O48**	2.07	μ_3-oxo
O11	2.10	μ_4-oxo	**O30**	2.03	μ_4-oxo	**O49**	2.05	μ_3-oxo
O12	2.12	μ_4-oxo	**O31**	2.03	μ_4-oxo	**O50**	2.09	μ_3-oxo
O13	2.04	μ_3-oxo	**O32**	2.14	μ_4-oxo	**O51**	0.40	H_2O
O14	2.10	μ_3-oxo	**O33**	2.15	μ_4-oxo	**O52**	0.32	H_2O
O15	2.03	μ_3-oxo	**O34**	2.02	μ_4-oxo	**O53**	0.35	H_2O
O16	2.04	μ_3-oxo	**O35**	2.12	μ_4-oxo	**O54**	0.27	H_2O

O17	2.06	μ_3-oxo	**O36**	2.14	μ_4-oxo	**O55**	0.35	H_2O
O18	0.53	H_2O	**O37**	2.06	μ_3-oxo			
O19	2.10	μ_3-oxo	**O38**	0.32	H_2O			

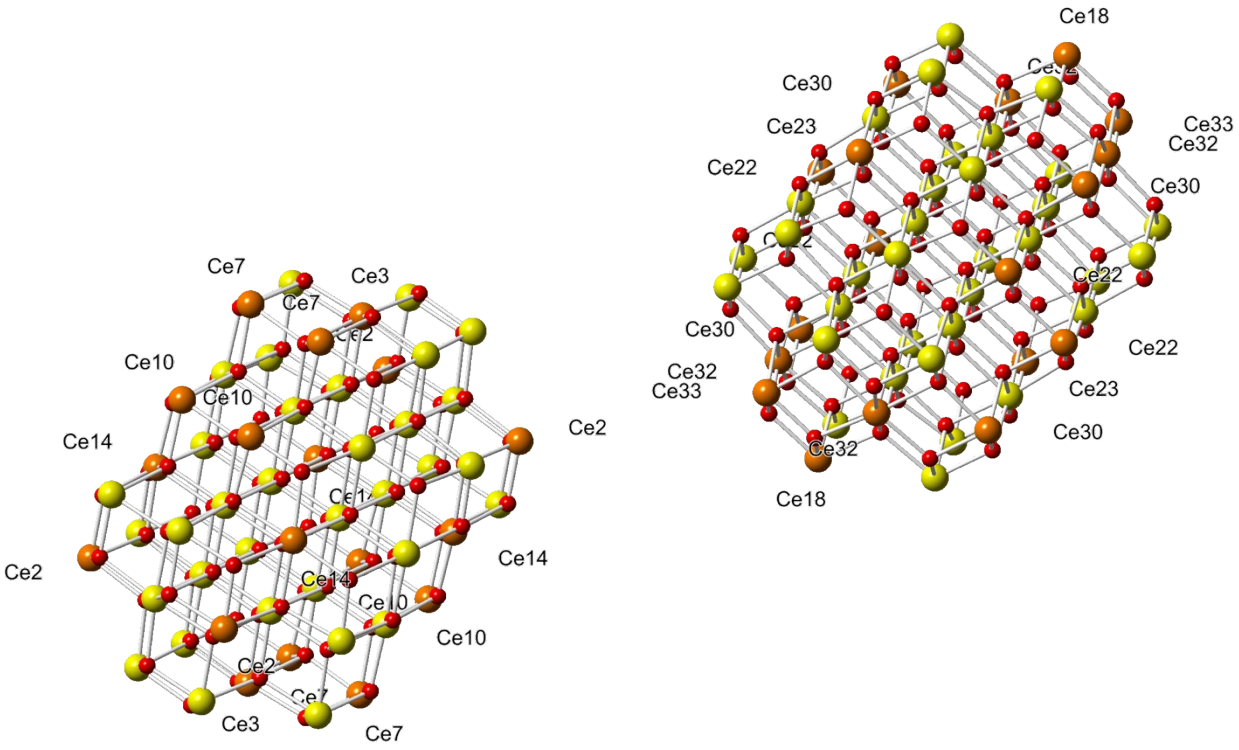

Figure S10. Illustration of the cluster cores of **Ce52** with proposed Ce sites that have both Ce^{III}/Ce^{IV} contribution in orange and Ce^{IV} sites in yellow. The Cl^- and H_2O ligands were omitted for clarity.

Bond Angle Comparison

In an effort to discern the μ_3-O sites as O^{2-} or OH^-, we compared the Ce-μ_3O-Ce bond angles of Ce38 and Ce52 with the Ce-μ_3O-Ce and Ce-μ_3(OH)-Ce for $[Ce_6O_4(OH)_4(dmb)_{12}(H_2O)_4]$.[8] For the hexamer, the Ce-μ_3O-Ce bond angles had an average of 117.46° and the Ce-μ_3(OH)-Ce bond angles had an average of 103.25°. These values show a clear difference between bond angles corresponding to a central O^{2-} or OH^-. Looking at the bond angles for Ce38, for each μ_3-O site, the bond angles ranged from ~108° - ~113°. A similar observation was made for the bond angles in Ce52, where the bond angles for a μ_3-O site could range from ~108° - ~114°. Bond angles for the hexamer reported by Christou et al, Ce38, and Ce52 are provided in Table S10. Additionally, Figures S11 and S12 show the bond angles for one μ_3-O site in Ce38 and Ce52, respectively. The bond angle values in Ce38 and Ce52 display ambiguity, unlike in the hexamer where the values are distinct between a Ce-μ_3O-Ce and a Ce-μ_3(OH)-Ce, that could be attributed to sites that are both O^{2-} and OH^-.

Table S10. Ce-μ_3O/OH-Ce bond angles for $[Ce_6O_4(OH)_4(dmb)_{12}(H_2O)_4]$, Ce38, and Ce52.

	Site	Angle 1	Angle 2	Angle 3	Average bond angle
$[Ce_6O_4(OH)_4(dmb)_{12}(H_2O)_4$	OH1	103.94	103.60	102.40	103.31
	OH2	101.70	105.02	102.15	102.96
	OH3	105.02	101.63	100.32	102.32
	OH4	104.64	104.38	104.25	104.43
	O1	118.75	118.27	114.90	117.31
	O2	117.49	119.24	117.61	118.12
	O3	117.95	119.73	114.37	117.35
	O4	118.54	117.42	115.24	117.07
Ce38	O8	107.90	113.13	111.98	111.00
	O10	112.30	112.05	107.94	110.76
	O11	108.35	112.31	112.31	110.99
	O13	108.48	112.29	112.82	111.19
	O15	107.92	112.63	112.80	111.11
	O16	112.84	112.54	108.78	111.39
	O17	112.68	108.99	112.46	111.38
	O19	107.63	113.19	111.90	110.91
	O20	108.03	112.01	112.51	110.85
	O28	112.12	113.32	108.17	111.20
	O30	108.02	111.77	113.24	111.01
	O36	112.61	113.08	108.86	111.51
Ce52	O13	110.92	110.92	107.76	109.87
	O14	110.74	114.54	108.84	111.37
	O15	110.90	110.90	107.81	109.87
	O16	111.14	108.96	113.05	111.05
	O17	107.10	111.81	112.74	110.55
	O19	108.97	112.69	110.62	110.76
	O21	114.03	111.19	113.56	112.92
	O24	108.19	109.88	110.80	109.62
	O49	108.35	110.84	114.52	111.24

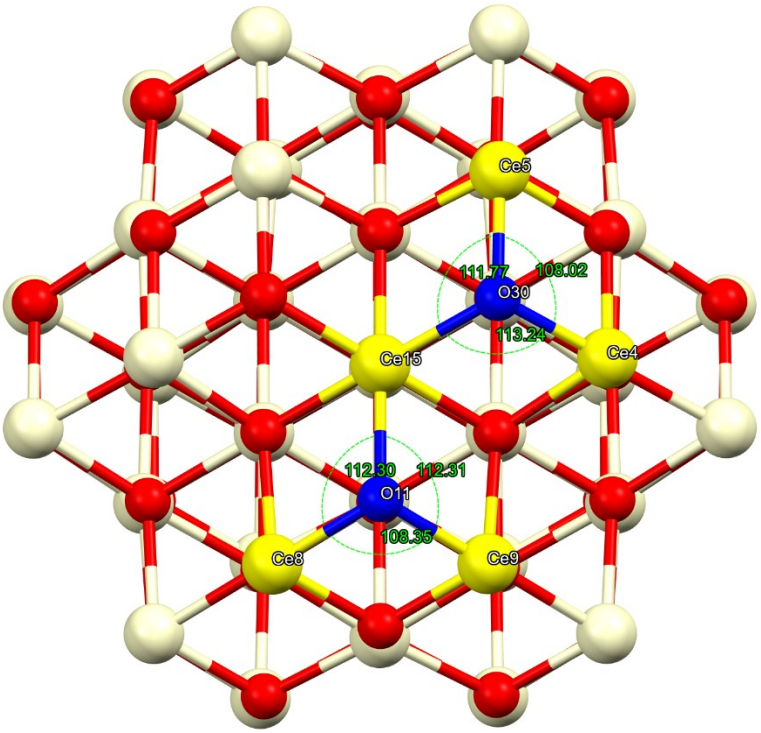

Figure S11. Illustration of Ce38 showing the Ce-μ_3O-Ce bond angles for O11 and O30. Cerium and oxygen atoms participating in the bond angles depicted are shown in yellow and blue, respectively. The bond angles are depicted in green.

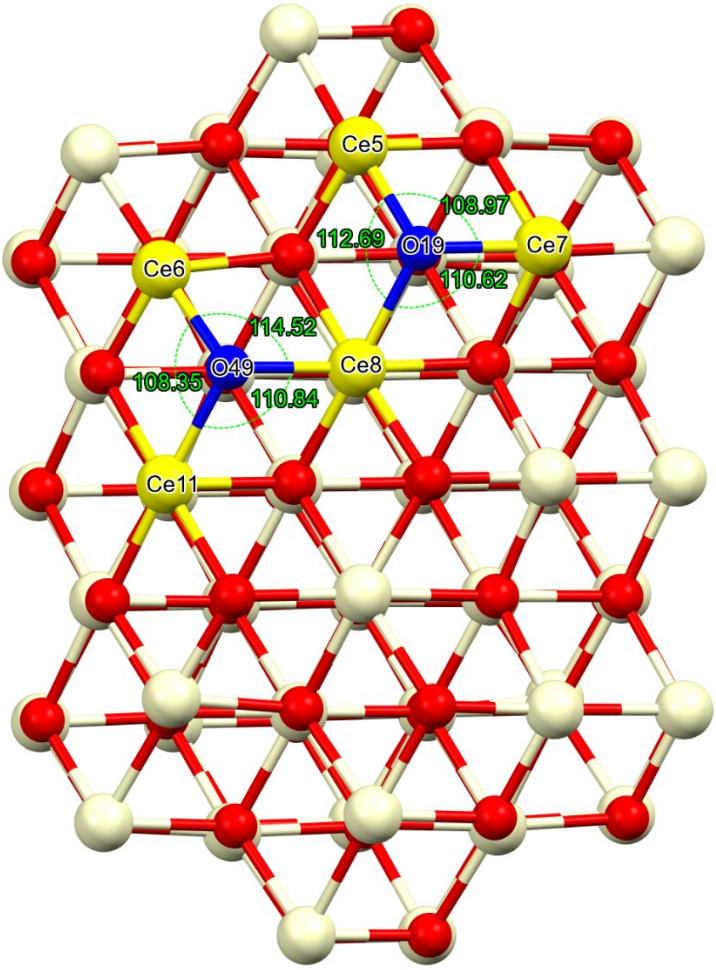

Figure S12. Illustration of Ce52 showing the Ce-μ_3O-Ce bond angles for O19 and O49. Cerium and oxygen atoms participating in the bond angles depicted are shown in yellow and blue, respectively. Bond angles are depicted in green.

H-bonding discussion

N-H---Cl donor-acceptor distances and angles were assessed using Platon to identify the presence of hydrogen bonding interactions in Ce1-1, Ce1-2, and Ce38. Since no pyridinium ions were modeled for Ce52, it is not included in this discussion. Potential H-bonding interactions were only present in Ce1-1 and Ce38 (Table S11).[9] In Ce1-1, H-bonding interactions exist between the outer sphere chloride and pyridinium ions. For Ce38, weak hydrogen bonding between a lattice water molecule and pyridinium is observed. Notably, no significant H-bonding interactions between the cluster surface and the HPy are present.

Table S11. Acceptor-donor bond distances for Ce1-1 and Ce38. No H-bonding present in these compounds.

Ce1-1		∠
Interaction	Distance (Å)	Angle (°)
	D-H --- A	D-H --- A
N(2B)-H--Cl(4)	2.96(10)	176(12)
N(2B)-H--Cl(4B)	2.977(11)	166(8)
Ce38		∠
Interaction	Distance (Å)	Angle (°)
	D-H --- A	D-H --- A
N(1)-H--O(37)	2.8(3)	171
N(2B)-H--Cl(19)	3.33(2)	120

Vibrational Spectroscopy

The Raman spectrum for a single crystal of **Ce52** was collected on a Horiba LabRAM HR Evolution Raman Microscope using a 532 nm laser over the 200 – 2000 cm^{-1} range.

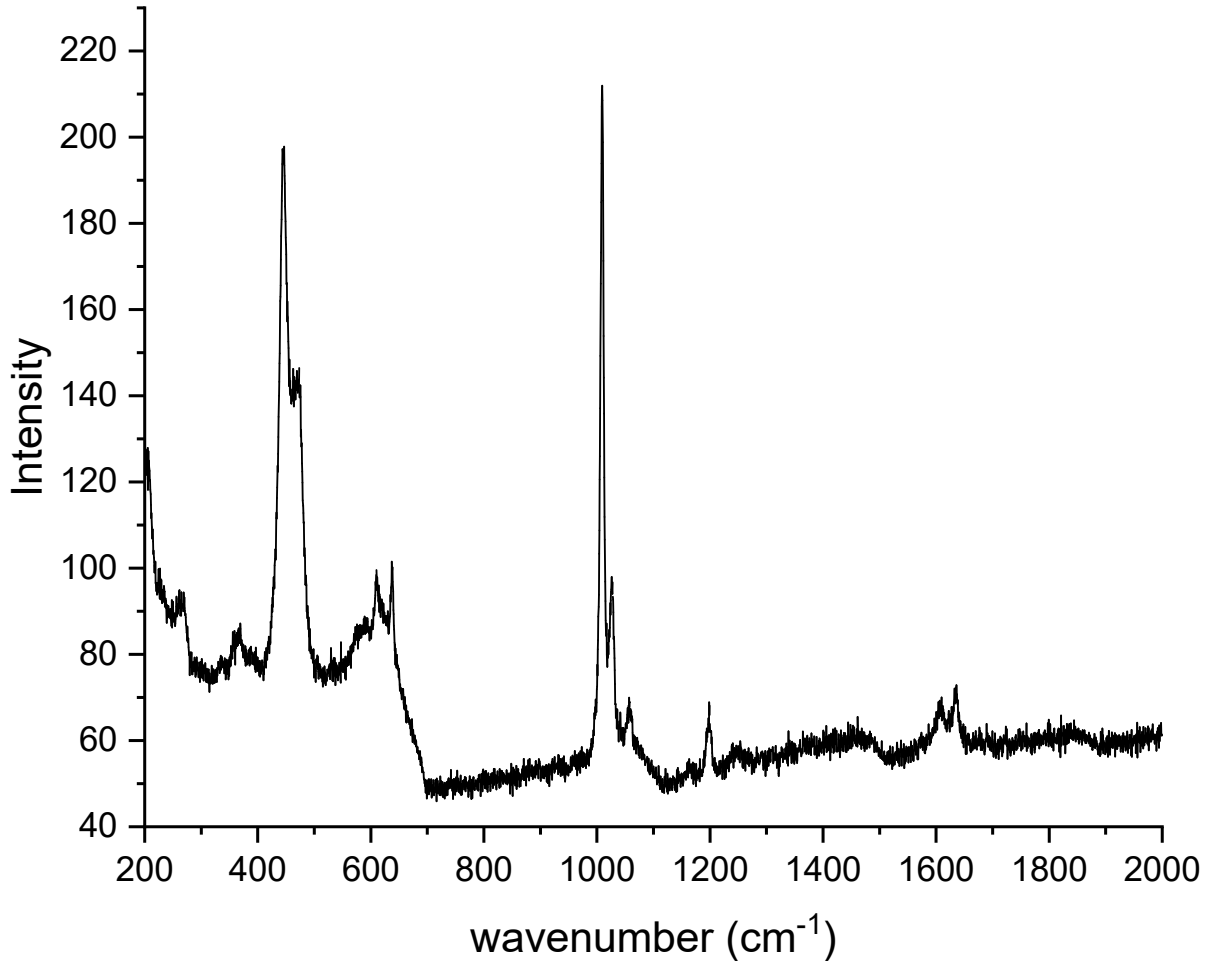

Figure S13. Raman spectrum of **Ce52** obtained in the 200 – 2000 cm^{-1} range using a 532 nm laser.

Table S12. Assignments for the Raman peaks in the spectrum for **Ce52**. Evidence of Ce-Cl, Ce-O and pyridinium are present in the spectrum.[4, 10-12]

Peak (cm^{-1})	**Assignment**
269.05	Ce-OH_2
366.41	Ce-Cl (potentially)
446.45	Ce-μ_3-O
473.24	Ce-μ_4-O
609.42	pyridine ring deformation or Ce defect mode
637.46	Pyridine
1009.42	Pyridine
1027.77	pyridine ring breathing
1058.38	pyridine
1199.4	pyridine ring stretch
1603.85	pyridine
1632.26	pyridine

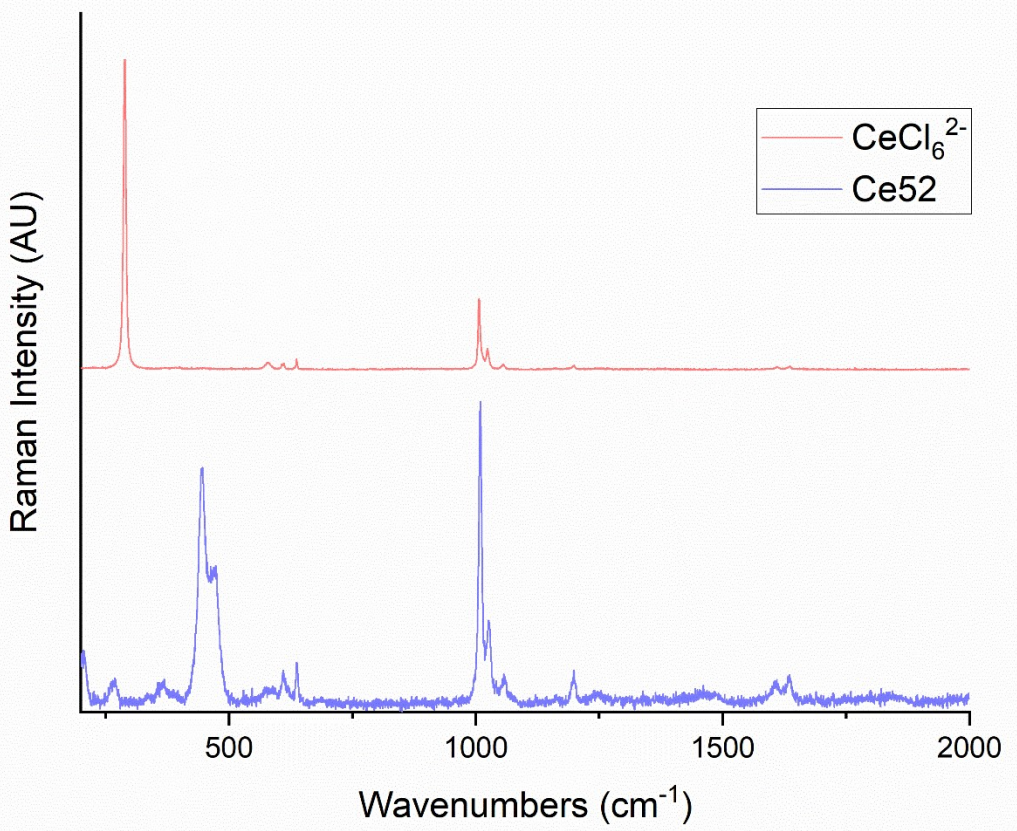

Figure S14. Raman spectra of **Ce52** and **$CeCl_6^{2-}$** obtained in the 200 – 2000 cm^{-1} range using a 532 nm laser.

The Raman spectra for **Ce52** and **$CeCl_6^{2-}$** showed overlapping peaks between 900 – 1250 cm^{-1}. These peaks are attributed to pyridinium stretches.

UV-vis-NIR electronic absorption spectroscopy

The UV-vis-NIR spectrum for **Ce52** was collected using a Craic UV-vis-NIR spectrometer. Data were collected over 200 – 1200 nm with an average of 35 scans. Bulk single crystals were used for the measurements.

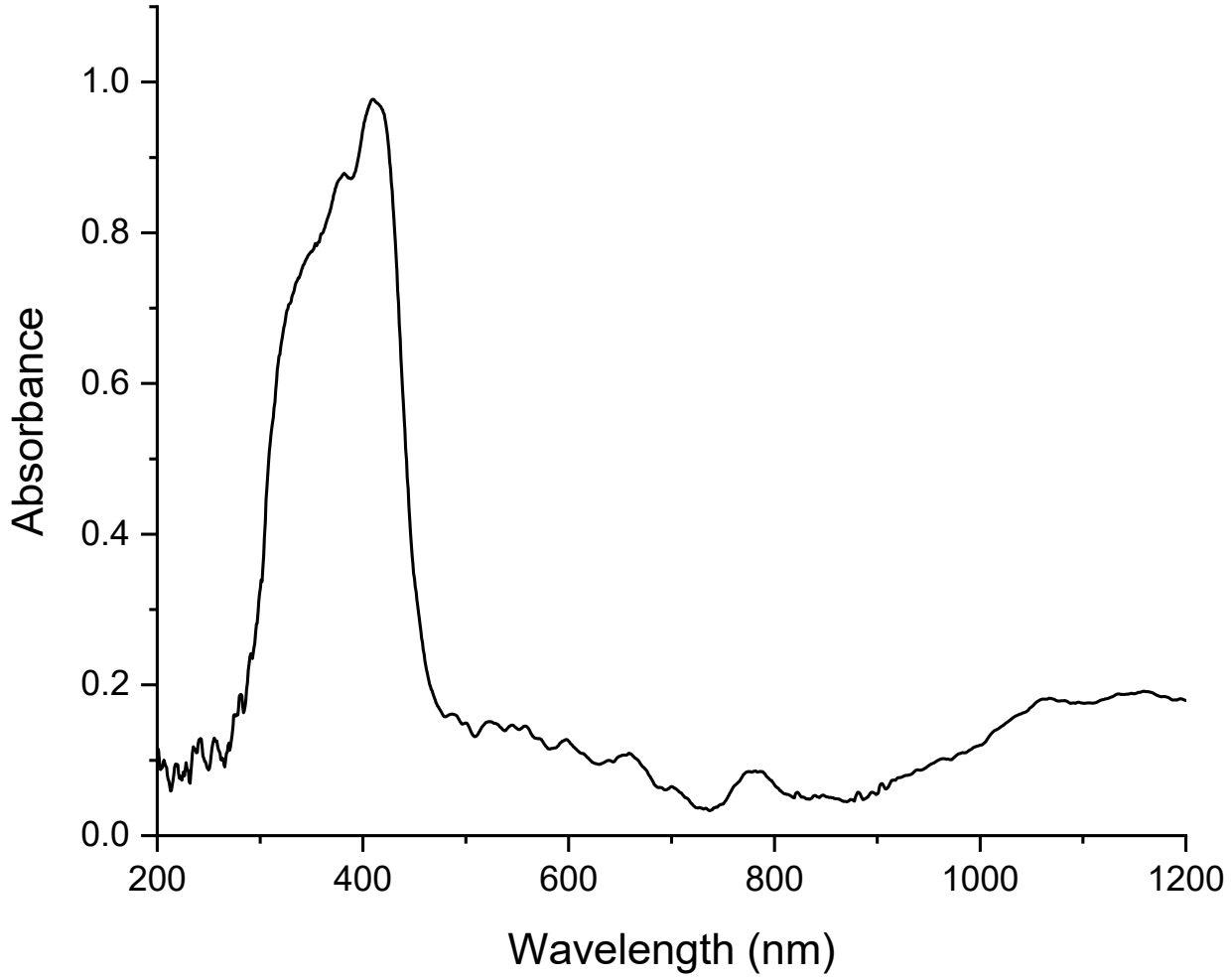

Figure S15. UV-vis-NIR spectrum for **Ce52** collected in the 200 – 1200 nm range. The band centered around 1100 nm is indicative of an intervalence charge transfer band.

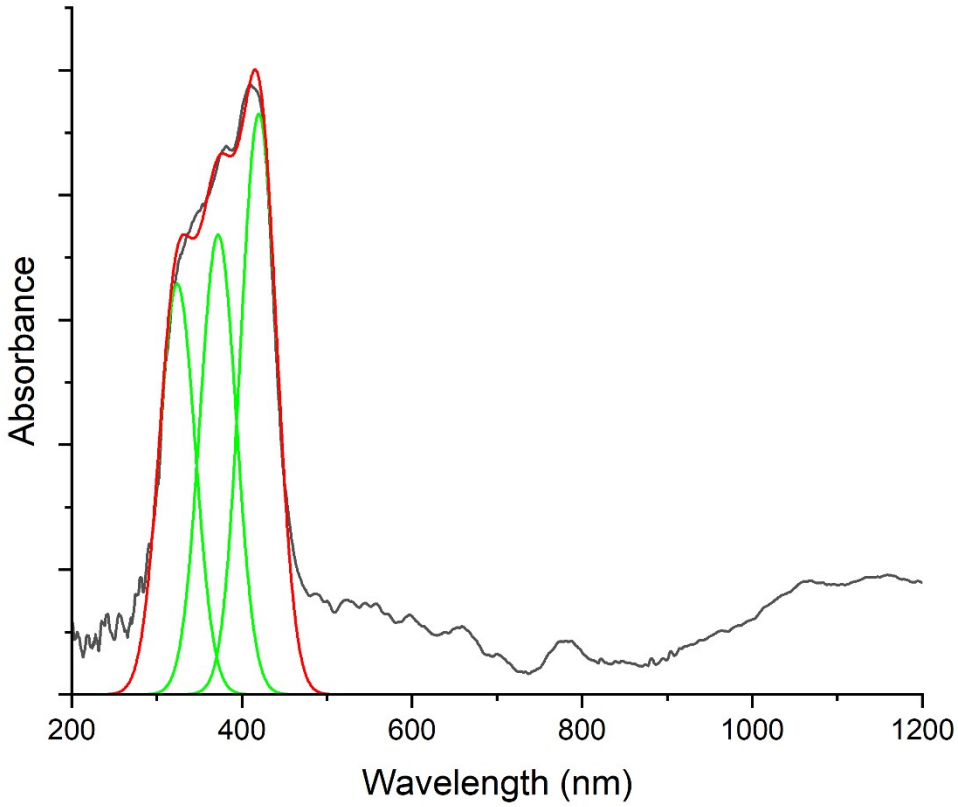

Figure S16. The peak centered around 400 nm in the UV-vis-NIR spectrum of **Ce52** was fit using a Lorenz-Gauss model in OriginPro.

REFERENCES

1. Bruker. *APEX3, SADABS, SAINT, SHELXTL, XCIF, XPREP*, Bruker AXS, Inc.: Madison, Wisconsin, USA, 2016.

2. Sheldrick, G. M., Crystal structure refinement with SHELXL. *Acta Cryst. C* **2015,** *71* (1), 3-8.

3. Hübschle, C. B.; Sheldrick, G. M.; Dittrich, B., ShelXle: a Qt graphical user interface for SHELXL. *J. Appl. Cryst.* **2011,** *44*, 1281-1284.

4. Wacker, J. N.; Ditter, A. S.; Cary, S. K.; Murray, A. V.; Bertke, J. A.; Seidler, G. T.; Kozimor, S. A.; Knope, K. E., Reactivity of a Chloride Decorated, Mixed Valent $Ce^{III/IV38}$–Oxo Cluster. *Inorg Chem* **2022,** *61* (1), 193-205.

5. Roulhac, P. L.; Palenik, G. J., Bond Valence Sums in Coordination Chemistry. The Calculation of the Oxidation State of Cerium in Complexes Containing Cerium Bonded Only to Oxygen. *Inorg. Chem.* **2003,** *42*, 118-121.

6. Brese, N. E.; O'Keeffe, M., Bond-Valence Parameters for Solids. *Acta Cryst.* **1991,** *B47*, 192-197.

7. Trzesowska, A.; Kruszynski, R.; Bartczak, T. J., Bond-valence parameters of lanthanides. *Acta Cryst. B* **2006,** *62* (Pt 5), 745-53.

8. Mitchell, K. J.; Goodsell, J. L.; Russell-Webster, B.; Twahir, U. T.; Angerhofer, A.; Abboud, K. A.; Christou, G., Expansion of the Family of Molecular Nanoparticles of Cerium Dioxide and Their Catalytic Scavenging of Hydroxyl Radicals. *Inorg. Chem.* **2021,** *60* (3), 1641-1653.
9. Steiner, T., The hydrogen bond in the solid state. *Angew. Chem. Int. Ed. Engl.* **2002,** *41* (1), 49-76.
10. Zhao; Jensen, L.; Schatz, G. C., Pyridine−Ag_{20} Cluster: A Model System for Studying Surface-Enhanced Raman Scattering. *J. Am. Chem. Soc.* **2006,** *128* (9), 2911-2919.
11. Arenas, J. F.; Woolley, M. S.; Otero, J. C.; Marcos, J. I., Charge-Transfer Processes in Surface-Enhanced Raman Scattering. Franck−Condon Active Vibrations of Pyrazine. *J. Phys. Chem.* **1996,** *100* (8), 3199-3206.
12. Wu, D. Y.; Hayashi, M.; Lin, S. H.; Tian, Z. Q., Theoretical differential Raman scattering cross-sections of totally-symmetric vibrational modes of free pyridine and pyridine–metal cluster complexes. *Spectrochim. Acta A Mol. Biomol. Spectrosc.* **2004,** *60* (1), 137-146.